

Syntheses, Photophysics, and Fluxional Properties of Luminescent A-Frame Diplatinum(II) Acetylide Complexes

Vivian Wing-Wah Yam,^{*,†} Phyllis Kok-Yan Yeung,[†] Lai-Ping Chan,[†]
Wai-Ming Kwok,[†] David Lee Phillips,^{*,†} Ka-Lai Yu,[†] Rick Wai-Kwok Wong,[‡]
Hong Yan,[§] and Qing-Jin Meng[§]

Department of Chemistry, The University of Hong Kong, Pokfulam Road, Hong Kong,
Department of Chemistry, Hong Kong Baptist University, Waterloo Road,
Kowloon, Hong Kong, and State Key Laboratory of Coordination Chemistry, Nanjing
University, Nanjing 210093, P. R. China

Received November 19, 1997

A series of A-frame Pt(II) acetylide complexes $[\text{Pt}_2(\mu\text{-dppm})_2(\mu\text{-C}\equiv\text{CR})(\text{C}\equiv\text{CR})_2]^+$ (R = C₆H₅, C₆H₄OMe-*p*, C₆H₄OEt-*p*, C₆H₄Et-*p*, Bp, ^tBu) have been isolated and shown to exhibit strong luminescence in both the solid state and in fluid solution. All these A-frame acetylide complexes have been found to exhibit fluxional properties. The free energies of activation for the fluxional process of selected Pt(II) A-frame acetylide complexes have been determined.

Introduction

Reactivity and fluxional properties of A-frame complexes have been main areas of interest for the past few decades.¹ Studies on the luminescent properties of d⁸–d⁸ A-frame complexes were rare. The first study on luminescent A-frame complexes was that of the pyrazolyl-bridged Rh(I) and Ir(I) dimers,² while most studies on d⁸–d⁸ dimers were confined to those geometries having stacked face-to-face square planes.³ Recently, A-frame platinum(II) acetylide complexes have been reported by us to possess long-lived excited states and are strongly emissive both in the solid state and in fluid

solution.⁴ Herein are reported a systematic spectroscopic study on a series of related complexes $[\text{Pt}_2(\mu\text{-dppm})_2(\mu\text{-C}\equiv\text{CR})(\text{C}\equiv\text{CR})_2]^+$, by which a variation in the nature of the acetylide ligands provides insights into the nature of the lowest-lying excited state (Chart 1). Moreover, these A-frame acetylide complexes have been found to exhibit fluxional properties similar to those complexes having the Pt₂(dppm)₂ unit.⁵ The free energies of activation for these processes of selected Pt(II) A-frame acetylide complexes have been determined.

Experimental Section

Materials and Reagents. The ligands bis(diphenylphosphino)methane (dppm), (*p*-methoxyphenyl)acetylene, (*p*-ethoxyphenyl)acetylene, (*p*-ethylphenyl)acetylene, biphenylacetylene, and Pt(cod)Cl₂ were purchased from Strem Chemicals Inc. [Pt-(dppm-*P,P'*)₂]Cl₂ was prepared by the literature method.⁶ Both acetonitrile and dichloromethane were purified and distilled using standard procedures before use.⁷ The pyridinium salts for quenching studies were prepared by refluxing the substituted pyridine with the corresponding alkylating reagent such as methyl iodide in acetone-ethanol (1:1, v/v) for 4 h, followed by metathesis in water using ammonium hexafluorophosphate and subsequent recrystallization from acetonitrile–diethyl ether. Tetra-*n*-butylammonium hexafluorophosphate (^tBu₄NPF₆) (Aldrich, 98%) was purified by twice recrystallization from absolute ethanol and dried under vacuum for 24 h before use. $[\text{Pt}_2(\mu\text{-dppm})_2(\text{C}\equiv\text{CC}_6\text{H}_5)_3]\text{ClO}_4$ (**5**)⁴ and $[\text{Pt}_2(\mu\text{-dppm})_2$

[†] The University of Hong Kong.

[‡] Hong Kong Baptist University.

[§] Nanjing University.

(1) Colton, R.; McCormick, M. J.; Dannan, C. D. *Aust. J. Chem.* **1978**, *31*, 1425. (b) Rattray, A. D.; Sutton, D. *Inorg. Chim. Acta* **1978**, *27*, L85. (c) Langrick, C. R.; McEwan, D. M.; Pringle, P. G.; Shaw, B. L. *J. Chem. Soc., Dalton Trans.* **1983**, 2487.

(2) Marshall, J. L.; Hopkins, M. D.; Miskowski, V. M.; Gray, H. B. *Inorg. Chem.* **1992**, *31*, 5034.

(3) (a) Roundhill, D. M.; Gray, H. B.; Che, C. M. *Acc. Chem. Res.* **1989**, *22*, 55 and references therein. (b) Fordyce, W. A.; Crosby, G. A. *J. Am. Chem. Soc.* **1982**, *102*, 985. (c) Miskowski, V. M.; Nobinger, G. L.; Klinger, D. S.; Hammond, G. S.; Lewis, N. S.; Mann, K. R.; Gray, H. B. *J. Am. Chem. Soc.* **1978**, *100*, 485. (d) Lewis, N. S.; Mann, K. R.; Gordon, J. G., II; Gray, H. B. *J. Am. Chem. Soc.* **1976**, *98*, 7461. (e) Che, C. M.; Yam, V. W. W.; Wong, W. T.; Lai, T. F. *Inorg. Chem.* **1989**, *28*, 758. (f) Che, C. M.; Butler, L. G.; Gray, H. B. *J. Am. Chem. Soc.* **1981**, *103*, 7796. (g) Fordyce, W. A.; Brummer, J. G.; Crosby, G. A. *J. Am. Chem. Soc.* **1981**, *103*, 7061. (h) Che, C. M.; Atherton, S. J.; Butler, L. G.; Gray, H. B. *J. Am. Chem. Soc.* **1984**, *106*, 5143. (i) Cho, K. C.; Che, C. M. *Chem. Phys. Lett.* **1986**, *124*, 313. (j) King, C.; Auerbach, R. A.; Fronczek, F. R.; Roundhill, D. M. *J. Am. Chem. Soc.* **1986**, *108*, 5626. (k) Roundhill, D. M.; Atherton, S. J. *J. Am. Chem. Soc.* **1986**, *108*, 6829. (l) Che, C. M.; Gray, H. B.; Atherton, S. J.; Lee, W. M. *J. Phys. Chem.* **1986**, *90*, 6747. (m) Marshall, J. L.; Hopkins, M. D.; Miskowski, V. M.; Gray, H. B. *Inorg. Chem.* **1992**, *31*, 5034. (n) Balch, A. L. *J. Am. Chem. Soc.* **1976**, *98*, 8049. (o) Milder, S. J.; Goldbeck, R. A.; Klinger, D. S.; Gray, H. B. *J. Am. Chem. Soc.* **1980**, *102*, 6761. (p) Che, C. M.; Lee, W. M.; Kwong, H. L.; Yam, V. W. W.; Cho, K. C. *J. Chem. Soc., Dalton Trans.* **1990**, 1717. (q) Mann, K. R.; Lewis, N. S.; Williams, R. M.; Gray, H. B.; Gordon, J. G., II *Inorg. Chem.* **1978**, *17*, 828. (r) Sacksteder, L.; Baralt, E.; DeGraff, B. A.; Lukehart C. M.; Demas, J. N. *Inorg. Chem.* **1991**, *30*, 3955.

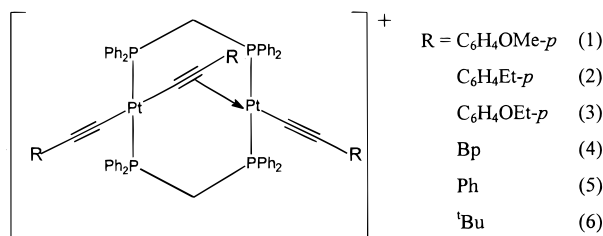
(4) Yam V. W. W.; Chan L. P.; Lai, T. F. *Organometallics* **1993**, *12*, 2197.

(5) Puddephatt, R. J.; Azam, K. A.; Hill, R. H.; Brown, M. P.; Nelson, C. D.; Moulding R. P.; Seddon K. R.; Gossel, M. C. *J. Am. Chem. Soc.* **1983**, *105*, 5642.

(6) Brown, M. P.; Fisher, J. R.; Hill, R. H.; Puddephatt, R. J.; Seddon, K. R. *Inorg. Chem.* **1981**, *20*, 3516.

(7) Perrins, D. D.; Armarego, W. L. F.; Perrin, D. R. *Purification of Laboratory Chemicals*, 2nd ed.; Pergamon Press: Oxford, U.K., 1980.

Chart 1



(C≡C^tBu)₃ClO₄ (**6**)⁸ were prepared according to literature methods. All other solvents and reagents were of analytical grade and were used as received.

Syntheses of Platinum(II) Complexes. [Pt₂(μ-dppm)₂(C≡CC₆H₄OMe-*p*)₃]ClO₄ (1**).** (*p*-Methoxyphenyl)acetylene (26 mg, 0.197 mmol) was added to a solution of mercury(II) acetate (30.8 mg, 0.097 mmol) in ethanol and the resultant solution added to a solution of Pt(dppm)₂Cl₂ (100 mg, 0.097 mmol) in ethanol (10 mL). The mixture was then heated under reflux for 24 h, cooled, and filtered. The orange filtrate was evaporated to dryness under reduced pressure. The residue was extracted with dichloromethane, which was then filtered, and upon addition of diethyl ether to the filtrate, orange crystals of [Pt₂(μ-dppm)₂(C≡CC₆H₄OMe-*p*)₃]Cl were obtained. Metathesis reaction to yield the ClO₄⁻ salt could be accomplished by dissolving the Cl⁻ salt in methanol, followed by addition of lithium perchlorate. Crystalline samples were obtained by recrystallization via slow diffusion of diethyl ether vapor into an acetonitrile solution of the complex. Yield: 30 mg (38%). ¹H NMR (CD₃CN): δ 3.63 (s, 6H, *terminal MeO*-), 3.77 (s, 3H, *bridging MeO*-), 4.51 (m, 2H, *H^β* (equatorial proton)), 4.57 (m, 2H, *H^α* (axial proton)), 6.30–8.00 (m, 52H, phenyl protons). ³¹P NMR (CD₃CN): δ 3.81 (s, *J*(P–Pt) = 2428 Hz). ¹⁹⁵Pt NMR (CD₂Cl₂): δ -4608 ppm (t, *J*(P–Pt) = 2425 Hz). IR (Nujol mull; ν/cm⁻¹ (C≡C)): 2117 w, 1995 w. FT-Raman (solid; ν/cm⁻¹ (C≡C)): 2122 s, 2043 w, 1995 s. UV/vis (MeCN; λ/nm (ε_{max}/dm³ mol⁻¹ cm⁻¹)): 262 (47 000), 408 (20 170), 450 (14 690). Anal. Calc for [Pt₂(μ-dppm)₂(C≡CC₆H₄OMe-*p*)₃]ClO₄: C, 56.0; H, 4.0. Found: C, 56.0; H, 4.0.

[Pt₂(μ-dppm)₂(C≡CC₆H₄Et-*p*)₃]PF₆ (2**).** The procedure is similar to that described for the preparation of **1** except (*p*-ethylphenyl)acetylene was used in place of (*p*-methoxyphenyl)acetylene. Recrystallization using CH₃CN/diethyl ether gave air-stable orange crystals of **2**. Yield: 43 mg (52%). ¹H NMR (CD₃CN): δ 1.10 (m, 9H, CH₃CH₂-), 2.50 (m, 6H, CH₃CH₂-), 4.50 (m, 2H, *H^β*), 4.58 (m, 2H, *H^α*), 6.30–8.00 (m, 52H, phenyl protons). ³¹P NMR (CD₃CN): δ 3.53 (s, *J*(P–Pt) = 2433 Hz). ¹⁹⁵Pt NMR (CD₂Cl₂): δ -4591 ppm (t, *J*(P–Pt) = 2410 Hz). IR (Nujol mull; ν/cm⁻¹ (C≡C)): 2125 w, 2007 w. FT-Raman (solid; ν/cm⁻¹ (C≡C)): 2124 s, 2030 w, 2007 s. UV/vis (MeCN; λ/nm (ε_{max}/dm³ mol⁻¹ cm⁻¹)): 262 (45 700), 398 (21 790), 440 (12 590). Anal. Calc for [Pt₂(μ-dppm)₂(C≡CC₆H₄Et-*p*)₃]PF₆: C, 56.9; H, 4.3. Found: C, 57.2; H, 4.4.

[Pt₂(μ-dppm)₂(C≡CC₆H₄OEt-*p*)₃]PF₆ (3**).** The procedure is similar to that described for the preparation of **1** except (*p*-ethoxyphenyl)acetylene was used in place of (*p*-methoxyphenyl)acetylene. Recrystallization using CH₃CN/diethyl ether gave air-stable orange crystals of **3**. Yield: 42 mg (50%). ¹H NMR (CD₃CN): δ 1.25 (t, 6H, *terminal CH₃CH₂O*-), 1.35 (t, 3H, *bridging CH₃CH₂O*-), 3.86 (q, 4H, *terminal CH₃CH₂O*-), 4.01 (q, 2H, *bridging CH₃CH₂O*-), 4.50 (m, 2H, *H^β*), 4.58 (m, 2H, *H^α*), 6.30–8.00 (m, 52H, phenyl). ³¹P NMR (CD₃CN): δ 3.79 (s, *J*(P–Pt) = 2428 Hz). ¹⁹⁵Pt NMR (CD₂Cl₂): δ -4582 ppm (t, *J*(P–Pt) = 2400 Hz). IR (Nujol mull; ν/cm⁻¹ (C≡C)): 2119 w, 1993 w. UV/vis (MeCN; λ/nm (ε_{max}/dm³ mol⁻¹ cm⁻¹)): 262 (49 150), 404 (30 160), 460 (16 140). Anal. Calc for [Pt₂(μ-dppm)₂(C≡CC₆H₄OEt-*p*)₃]PF₆: C, 55.2; H, 4.1. Found: C, 55.4; H, 4.0.

[Pt₂(μ-dppm)₂(C≡CBp)₃]PF₆ (4**).** The procedure is similar to that described for the preparation of **1** except biphenylacetylene was used in place of (*p*-methoxyphenyl)acetylene. Recrystallization using CH₃CN/diethyl ether gave air-stable orange crystals of **4**. Yield: 34 mg (39%). ¹H NMR (CD₃CN): δ 4.55 (m, 4H, *H^α* and *H^β*), 6.50–8.00 (m, 67H, phenyl protons). ³¹P NMR (CD₃CN): δ 3.71 (s, *J*(P–Pt) = 2402 Hz). ¹⁹⁵Pt NMR (CD₂Cl₂): δ -4609 ppm (t, *J*(P–Pt) = 2423 Hz). IR (Nujol mull; ν/cm⁻¹ (C≡C)): 2122 w, 2005 w. FT-Raman (solid; ν/cm⁻¹ (C≡C)): 2125 s, 2028 w, 2009 w. UV/vis (MeCN; λ/nm (ε_{max}/dm³ mol⁻¹ cm⁻¹)): 304 (60 980), 394 (20 360), 436 (14 560). Anal. Calc for [Pt₂(μ-dppm)₂(C≡CBp)₃]PF₆: C, 59.0; H, 4.1. Found: C, 59.1; H, 3.9.

Physical Measurements and Instrumentation. All infrared spectra were recorded as Nujol mull on KBr cells on either a Bio-Rad FTS-71R spectrophotometer (4000–400 cm⁻¹) or Shimadzu IR-470 infrared spectrophotometer (4000–400 cm⁻¹). ¹H, ¹³C, ³¹P, and ¹⁹⁵Pt NMR were recorded on either a Bruker AM-500 (500 MHz), Bruker DPX-300 (300 MHz), or JEOL JNM-GSX270 (270 MHz) multinuclear FT-NMR spectrometer. Chemical shifts (δ, ppm) were reported relative to tetramethylsilane (Me₄Si) for ¹H and ¹³C NMR, Na₂PtCl₄ in D₂O for ¹⁹⁵Pt, and 85% H₃PO₄ for ³¹P NMR, respectively. All UV-vis spectra were recorded on a HP8452A diode array spectrophotometer. Steady-state emission and excitation spectra at room temperature and at 77 K were obtained on a Spex Fluorolog-2 model F111 fluorescence spectrophotometer with or without Corning filters. The 77 K solid-state emission and excitation spectra were recorded with solid samples loaded in a quartz tube inside a quartz-walled optical Dewar flask filled with liquid nitrogen.

For solution emission and excitation spectral studies, the solutions were prepared in a 10 mL Pyrex bulb connected to a side-arm 1-cm quartz cuvette and sealed from the atmosphere by a Kontes quick release Teflon stopper. The solutions were degassed by no fewer than three freeze–pump–thaw cycles. Emission-lifetime measurements were performed using a conventional laser system. The excitation source was the 355 nm output (third harmonic) of a Quanta-Ray Q-switched GCR-150-10 pulsed Nd-YAG laser. Luminescence decay signals were recorded on a Tektronix model TDS620A digital oscilloscope and analyzed using a program for exponential fits. Elemental analyses of the newly synthesized complexes were performed by Butterworth Laboratories Ltd.

Quenching studies were performed using time-resolved lifetime measurements and the bimolecular quenching rate constants *k_q* determined according to the Stern–Volmer equation, τ₀/τ = 1 + *k_q*τ₀[Q], where τ₀ and τ are the excited-state lifetimes in the absence and in the presence of quencher at concentration [Q]. In each case, a linear plot of τ₀/τ versus quencher concentration, [Q] was obtained from which the quenching rate constant *k_q* was deduced.

The resonance Raman spectrum was obtained with an experimental apparatus and methods described previously.⁹ FT-Raman spectra were recorded on a Bio-Rad FT Raman spectrometer.

The fluxional behaviors of the complexes were studied by variable-temperature NMR spectroscopy using the Bruker AM-500 FT-NMR spectrometer.

The coalescence temperatures for the various signals and the corresponding Δ*G*[‡] values are estimated from the Eyring

(8) Alcock, N. W.; Kemp T. J.; Pringle, P. G.; Bergamini, P.; Traverso, O. *J. Chem. Soc., Dalton Trans.* **1987**, 1659.

(9) (a) Kwok, W. M.; Phillips, D. L.; Yeung, P. K. Y.; Yam, V. W. W. *Chem. Phys. Lett.* **1996**, *262*, 699. (b) Kwok, W. M.; Phillips, D. L.; Yeung, P. K. Y.; Yam, V. W. W. *J. Phys. Chem. A* **1997**, *101*, 9286.

equation^{10a}

$$\Delta G^\ddagger = RT_c \left(\ln \frac{k_B}{h} + \ln \frac{T_c}{k} \right)$$

where k is rate constant for the fluxional process and R , T_c , k_B , and h are the universal gas constant, coalescence temperature, Boltzmann constant, and Planck constant, respectively.

The method for the determination of the rate constant k is dependent on the type of fluxional system. For the methylene protons of dppm ligand, the two signals are equally populated and indicate a coupled two site exchange system; the rate constant is determined using the equation^{10a}

$$k = \pi(\delta\nu)/\sqrt{2}$$

For the acetylide ligands, the terminal and bridging acetylide signals are unequally populated and indicate an uncoupled two site exchange system; the rate constant k is determined according to the method of Lynden-Bell.^{10b-d}

$$k = \pi\{0.5[(\delta\nu)^2 + 6J_{\alpha\beta}^2]\}^{1/2}$$

where $\delta\nu$ is the difference in the chemical shift between protons α and β at very low exchange rate and $J_{\alpha\beta}$ is the coupling constant between protons α and β .

Results and Discussion

Although a number of hetero- and homobimetallic face-to-face platinum(II) acetylide complexes^{3r,11a-c} and binuclear d⁸-d⁸ A-frame complexes^{4,8,11d} were isolated, it was in 1987 that the first report on the isolation of a binuclear Pt(II) A-frame acetylide complex was published.⁸ Reaction of [Pt(dppm-*P,P*)Cl₂] with LiC≡C*Bu*^t in boiling tetrahydrofuran afforded the corresponding A-frame diplatinum acetylide complex. However, reaction of [Pt(dppm-*P,P*)Cl₂] under the same conditions with LiC≡C*R* (*R* = Ph or C₆H₄Me-*p*) did not produce the A-frame complexes. Instead the face-to-face dimers of [Pt₂(*μ*-dppm)₂(C≡C*R*)₄] were isolated.^{11c} The formation of the A-frame [Pt₂(*μ*-dppm)₂(*Bu*C≡C)₃]⁺ complex rather than [Pt₂(*μ*-dppm)₂(*Bu*C≡C)₄] has been attributed by Pringle and co-workers⁸ to the steric bulk as well as the electron richness of the *tert*-butyl group compared to the phenyl and the tolyl groups. It was only recently that the isolation of an analogous homobimetallic Pt(II) A-frame complex of the less bulky and less electron-rich phenylacetylide was reported by us.⁴ In this method, phenylacetylene was deprotonated by mercury(II) acetate to form the corresponding mercury phenylacetylide in ethanol, which was then reacted with Pt(dppm)₂Cl₂ in refluxing ethanol to yield the A-frame product in reasonable yield. The only side product was the heterobimetallic platinum-mercury complex [Pt(*μ*-dppm)₂(C≡C*R*)₂HgCl₂], which was not very soluble in

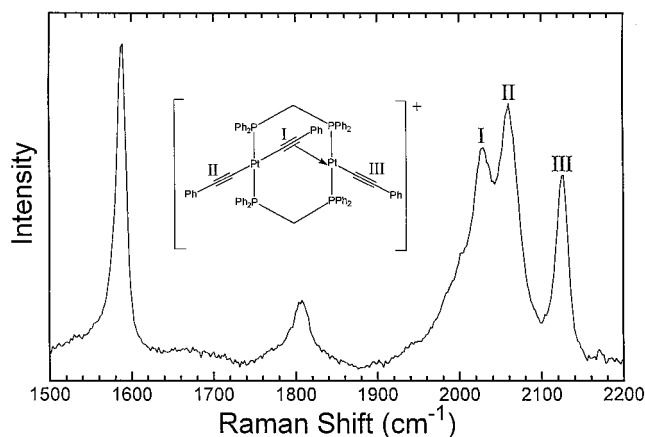


Figure 1. Resonance Raman spectrum of [Pt₂(*μ*-dppm)₂(C≡CPh)₃]⁺ in acetonitrile with excitation wavelength at 416 nm.

ethanol and could easily be separated from the chloride salt of the product by filtration.

This method appeared to be general and could be extended to accomplish other substituted phenylacetylide complexes such as those of (methoxyphenyl)-, (ethoxyphenyl)-, (ethylphenyl)- and biphenylacetylide. Two rather weak and ill-resolved IR bands in the 2000–2100 cm⁻¹ region were observed, which could be ascribed to the ν (C≡C) stretches. The lower ν (C≡C) stretching frequency at *ca.* 2000 cm⁻¹ in the IR spectra is ascribed to the μ - η^2 bridgehead acetylide group while the one at higher frequency (\sim 2100 cm⁻¹) is assigned to the terminal acetylide groups. On the other hand, three distinct ν (C≡C) stretches were observable at *ca.* 2125, 2062, and 2027 cm⁻¹ in both the FT-Raman and resonance Raman spectra,⁹ corresponding to the three different acetylide environments (Figure 1). The three acetylide Raman peaks shown in Figure 1 are consistent with the assignment of each of these Raman bands to the different acetylide environments. The observation of only two bands in the IR spectra is likely to arise as a result of the fact that either the third peak is too weak in intensity or is too close in frequency to the other two that it is not discernible. Similar stretching frequencies were also found for the bridging and terminal acetylides in complexes such as [NBu₄]₂[Pt₃(C₆F₅)₄(*μ*-C≡CPh)₄],^{12a} [NBu₄]₂[Pt₂Ag₂(C₆F₅)₄(C≡CPh)₄],^{12b} and [NBu₄]₂[*cis*-Pt-(C₆F₅)₂(C≡CSiMe₃)₂]₂HgBr₂].^{12c} All complexes gave satisfactory elemental analyses and were characterized by NMR spectroscopy.

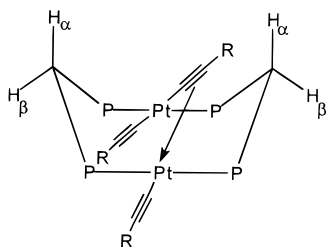
The room-temperature ¹H NMR spectra of complexes **1–6** all showed two broad multiplets at *ca.* 4.5–4.6, assigned as the methylene resonances of the dppm ligand. The observation of two broad multiplets is indicative of the nonequivalence of the methylene protons (H_α and H_β) on the NMR time scale (Chart 2). For complexes **1**, **3**, and **6**, apart from the observation of two sets of methylene signals, two sets of methoxy, ethoxy, and *tert*-butyl signals in the integral ratio of 2:1 are also observed, respectively, indicative of the nonequivalence of the acetylide ligands. A close scrutiny

(10) (a) Sandström, J. *Dynamic NMR Spectroscopy*; Academic Press: London, 1982. (b) Lynden-Bell, R. M. *Progress in NMR Spectroscopy*; Pergamon Press: New York, 1967; Vol. 2. (c) Shanani-Atidi, H.; Bar-Eli, K. H. *J. Phys. Chem.* **1970**, *74*, 961. (d) Mayr, A.; Asaro, M. F.; Glines, T. J.; Engen, D. V.; Tripp, G. M. *J. Am. Chem. Soc.* **1993**, *115*, 8187.

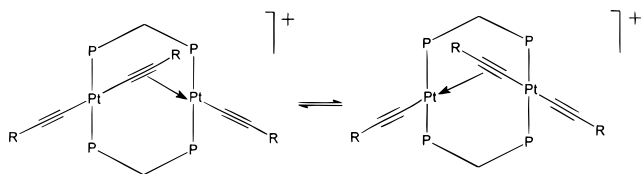
(11) (a) Cooper, G. R.; Hutton, A. T.; Langrick, C. R.; McEwan, D. M.; Pringle, P. G.; Shaw, B. L. *J. Chem. Soc., Dalton Trans.* **1984**, 855. (b) McDonald, W. S.; Pringle, P. G.; Shaw, B. L. *J. Chem. Soc., Chem Commun.* **1982**, 861. (c) Langrick, C. R.; McEwan, D. M.; Pringle, P. G.; Shaw, B. L. *J. Chem. Soc., Dalton Trans.* **1983**, 2487. (d) Blagg, A.; Hutton, A. T.; Pringle, P. G.; Shaw, B. L. *J. Chem. Soc., Dalton Trans.* **1984**, 1815.

(12) (a) Forniés, J.; Lalinde, E.; Martín, A.; Moresno, M. T. *J. Chem. Soc., Dalton Trans.* **1994**, 135. (b) Espinet, P.; Forniés, J.; Martínez, F.; Sotes, M. *J. Organomet. Chem.* **1991**, *403*, 253. (c) Berenguer, J. R.; Forniés, J.; Lalinde, E.; Martín, A.; Moreno, M. T. *J. Chem. Soc., Dalton Trans.* **1994**, 3343.

Chart 2



Scheme 1



of the structure of these A-frame complexes would predict three nonequivalent acetylide groups which should give rise to three sets of resonances in a 1:1:1 ratio instead of two sets in a 2:1 ratio.

In order to account for such an observation, it is likely that either two of the three acetylides have very similar chemical shifts or a σ,π -acetylide exchange process is in operation, rendering the two terminal acetylides equivalent (Scheme 1).

Such a σ,π -acetylide exchange process or "windscreen wiper" action has also been observed to occur readily in other μ -acetylide systems at room temperature^{8,13} and has also been suggested to account for the equivalence of both the ^{31}P and ^{195}Pt nuclei of complex **6**.⁸ The ^{31}P and ^{195}Pt NMR spectra of complexes **1–5** also showed a singlet and triplet, respectively, at *ca.* δ 3.6 and -4600 ppm, indicative of the equivalency of the ^{31}P and ^{195}Pt nuclei in the A-frame complexes at room temperature. It is interesting to note that unlike the Raman spectra, which show three nonequivalent acetylide environments, the NMR spectra indicate that there are two nonequivalent acetylide environments with a 2:1 ratio even upon cooling to -40 °C. Thus the proposed σ,π -acetylide exchange process (Scheme 1) should occur at a rate faster than the NMR time scale at -40 °C ($\sim 10^{-2}$ – 10^{-5} s) so as to give rise to equivalence of the two terminal acetylide groups and a different bridging acetylide group consistent with the 2:1 ratio of the NMR spectra. However, the σ,π -acetylide exchange process (Scheme 1) should occur at a rate slower than the vibrational time scale (10^{-12} – 10^{-13} s) in order to give three nonequivalent acetylide environments to be consistent with the resonance Raman and FT-Raman spectra which show three acetylide C \equiv C stretch peaks.

In order to investigate in more detail and to gain further insight into the fluxional behavior of the complexes, a variable-temperature ^1H NMR study was pursued. Similar to the previous report by Pringle and co-workers,⁸ upon lowering of the temperature to -40 °C, the CH_2 protons still remained inequivalent and

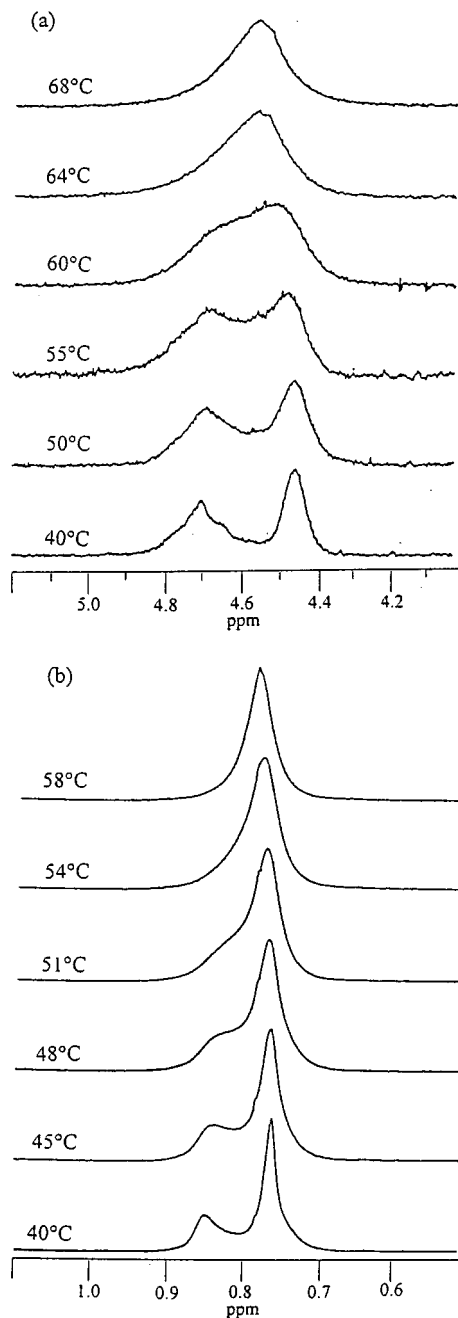


Figure 2. ^1H NMR spectra showing (a) the methylene protons of the dppm ligand and (b) the methyl protons of the *tert*-butyl acetylide ligand in $[\text{Pt}_2(\mu\text{-dppm})_2(\text{C}\equiv\text{C}^t\text{Bu})_3]\text{ClO}_4$ in CD_3CN at various temperatures.

Table 1. Activation Parameters and Coalescence Temperatures from Variable-Temperature ^1H NMR Studies of the Fluxional Processes of $[\text{Pt}_2(\mu\text{-dppm})_2(\text{C}\equiv\text{CR})_3]^+$ in CD_3CN

complex	coalescence temp (K) of the CH_2 resonance ($\Delta G^\ddagger/\text{kJ mol}^{-1}$)	coalescence temp (K) of the acetylide resonance ($\Delta G^\ddagger/\text{kJ mol}^{-1}$) ^a
1	314 (64.2)	321 (63.2)
3	320 (64.7)	320 (63.6)
6	330 (65.7)	321 (64.0)

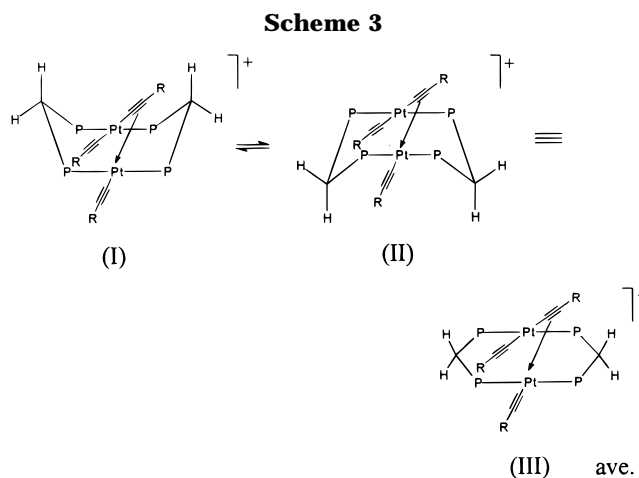
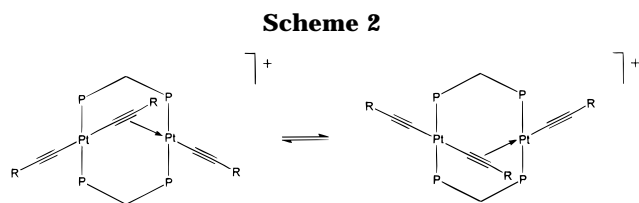
^a ΔG^\ddagger is the free energy of activation for the dynamic process (minor isomer form \rightarrow major isomer form).

showed an AB pattern while the acetylide signals still remained as two sets in a ratio of 2:1. On the other hand, upon raising of the temperature above room

(13) (a) Cherkas, A. A.; Randall, L. H.; MacLaughlin, S. A.; Mott, G. N.; Taylor, N. J.; Carty, A. J.; *Organometallics* **1988**, *7*, 969. (b) Top, S.; Gunn, M.; Jaouen, G.; Vaissermann, J.; Daran, J.-C.; McGlinchey, M. J. *Organometallics* **1992**, *11*, 1201. (c) Lee, K. W.; Pennington, W. T.; Cordes, A. W.; Brown, T. L. *J. Am. Chem. Soc.* **1985**, *107*, 631.

Table 2. Photophysical Data for $[\text{Pt}_2(\mu\text{-dppm})_2(\text{C}\equiv\text{CR})_3]^+$

complex	λ/nm ($\epsilon_{\text{max}}/\text{dm}^3 \text{ mol}^{-1} \text{ cm}^{-1}$) in MeCN	medium (TK)	$\lambda_{\text{em}}/\text{nm}$ ($\tau_0/\mu\text{s}$)
1	408 (20 170), 450 (14 690)	solid (298)	610 (10.0 \pm 0.5)
		MeCN (298)	630 (0.10 \pm 0.01)
2	398 (21 790), 440 (12 590)	CH_2Cl_2 (298)	635 (0.20 \pm 0.02)
		solid (298)	590 (11.0 \pm 0.5)
3	404 (30 160), 460 (16 140)	solid (77)	575, 645 sh
		MeCN (298)	620 (0.15 \pm 0.01)
4	394 (20 360), 436 (14 560)	CH_2Cl_2 (298)	630 (0.14 \pm 0.01)
		solid (298)	595 (9.0 \pm 0.5)
5^a	393 (18 170), 450 (7370)	solid (77)	575, 645 sh
		MeCN (298)	630 (0.15 \pm 0.01)
6	344 (6480), 375 sh (8100), 391 (8460), 410 sh (7190)	CH_2Cl_2 (298)	623 (<0.1)
		solid (298)	618 (2.2 \pm 0.2)
6	344 (6480), 375 sh (8100), 391 (8460), 410 sh (7190)	solid (77)	621
		MeCN (298)	614 (0.11 \pm 0.01)
6	344 (6480), 375 sh (8100), 391 (8460), 410 sh (7190)	CH_2Cl_2 (298)	623 (<0.1)
		solid (298)	554 (11.0 \pm 0.5)
6	344 (6480), 375 sh (8100), 391 (8460), 410 sh (7190)	solid (77)	565
		MeCN (298)	500 (<0.1)

^a From ref 4.

temperature, the separation between the two broad methylene signals decreases and finally coalesce to a single broad signal at 321 K. The ^1H NMR spectra of complex **6** at various temperature are shown in Figure 2. For complexes **1**, **3**, and **6**, apart from the observation of the coalescence of the methylene resonances at high temperatures, the *tert*-butyl signals of complex **6**, the methoxy signals of complex **1**, and the ethoxy signals of complex **3** for the bridging and terminal acetylide ligands also coalesce upon increasing the temperature. The coalescence temperatures for the various signals and the corresponding ΔG^\ddagger values estimated from the Eyring equation^{10a} are summarized in Table 1. Within experimental errors, the ΔG^\ddagger values ($\sim 65 \text{ kJ mol}^{-1}$) estimated from the methylene and the acetylide coalescences are similar or identical. Despite the approximations implicit in this method of estimating ΔG^\ddagger , the results suggest that the coalescences of the methylene and the acetylide resonances are related and may originate from the same fluxional process. The concurrent equilibration of the methylene protons and the acetylide units is likely to involve a bridging-to-terminal acetylide ligand exchange (Scheme 2).

It is noteworthy that both the structures of **5** and **6** showed a pseudoboat conformation (I), which have been confirmed by X-ray crystallography (Chart 2).^{4,8} The A-frame inversion for complexes of this conformation is usually accompanied by inversion of the pseudoboat or the so-called "flipping" process (Scheme 3).

It is likely that such flipping process is facile and occurs readily with very small activation energy, which could be viewed to give a time-averaged structure (III) with the $\text{Pt}_2\text{P}_4\text{C}_2$ unit lying on the same plane. It is believed that, at room temperature, both the σ,π -acetylide exchange (Scheme 1) and the pseudoboat

inversion (Scheme 3) processes are fast, leading to the equivalency of the two terminal acetylide protons but the inequivalency of the methylene protons due to the A-frame structure. However, at high temperatures, the bridging-to-terminal acetylide exchange (Scheme 2) occurs which led to the equivalency of both the acetylide ligands and the methylene protons. Thus the ΔG^\ddagger value obtained is that measured for the bridging-to-terminal acetylide exchange process. Attempts to evaluate the ΔG^\ddagger values for the other fluxional processes described in Schemes 1 and 3 are unsuccessful since, upon lowering of the temperature to -40°C in CD_3CN , no alteration in the NMR spectroscopic properties was observed. It is likely that these processes are fast even at -40°C . A similar ΔG^\ddagger value of 68 kJ mol^{-1} has also been estimated for the bridging-to-terminal ligand exchange in $[\text{Pt}_2\text{H}_2(\mu\text{-H})(\mu\text{-dppm})_2]^+$,¹⁴ which is higher than that of the A-frame inversion process in which a ΔG^\ddagger of 46.5 kJ mol^{-1} was reported by Puddephatt and co-workers.¹⁵ Several mechanisms for the A-frame inversion have been discussed in detail.¹⁵

(14) Brown, M. P.; Puddephatt, R. J.; Rashidi, M.; Seddon, K. R. *J. Chem. Soc., Dalton Trans.* **1978**, 516.

(15) Puddephatt, R. J.; Azam, K. A.; Hill, R. H.; Brown, M. P.; Nelson, C. D.; Moulding, R. P.; Seddon, K. R.; Grossel, M. C. *J. Am. Chem. Soc.* **1983**, *105*, 5642 and references therein.

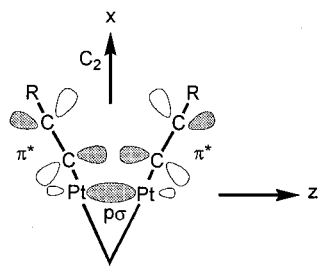


Figure 3. Schematic diagram showing the overlap between the p_{σ} orbital (resulting from $6p_z-6p_z$ orbital overlap) and the π^* orbital on the acetylide ligands.

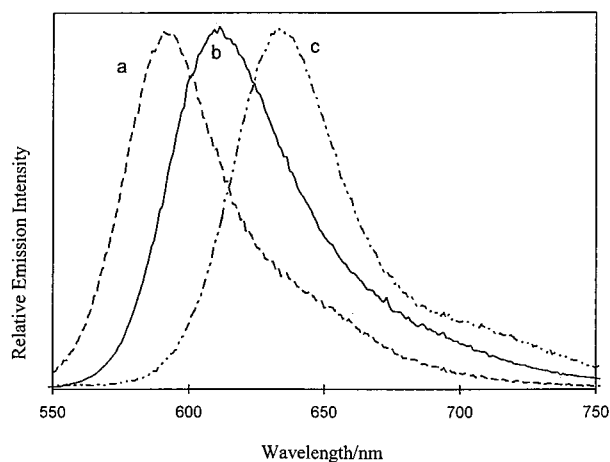


Figure 4. Normalized emission spectra of A-frame complexes in the solid state at room temperature: (a) $[\text{Pt}_2(\text{dppm})_2(\text{C}\equiv\text{CC}_6\text{H}_4\text{Et-}p)_3]\text{PF}_6$; (b) $[\text{Pt}_2(\text{dppm})_2(\text{C}\equiv\text{CC}_6\text{H}_4\text{OMe-}p)_3]\text{PF}_6$; (c) $[\text{Pt}_2(\text{dppm})_2(\text{C}\equiv\text{CBp})_3]\text{PF}_6$.

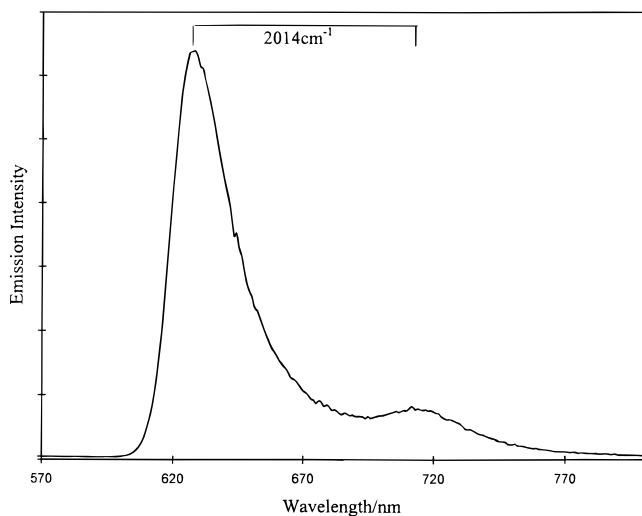


Figure 5. Solid-state emission spectrum of $[\text{Pt}_2(\mu\text{-dppm})_2(\text{C}\equiv\text{CBp})_3]\text{PF}_6$ at 77 K.

The electronic absorption spectra of complexes **1–4** and **6** both in acetonitrile and dichloromethane exhibit similar absorption patterns. Similar findings have also been observed for complex **5** recently.⁴ With reference to previous spectroscopic work on complex **5**⁴ and a related A-frame dinuclear Ir(I) system,² the absorption band centered at *ca.* 400 nm, like $[\text{Pt}_2(\mu\text{-dppm})_2(\text{C}\equiv\text{CC}_6\text{H}_5)_3]^+$ (**5**), is assigned as a MMLCT (metal-metal-bond-to-ligand charge transfer) [$d\sigma^* \rightarrow p\sigma/\pi^*$] transition, which has been red-shifted with respect to the MLCT (metal-to-ligand charge transfer) [$d \rightarrow \pi^*$ -

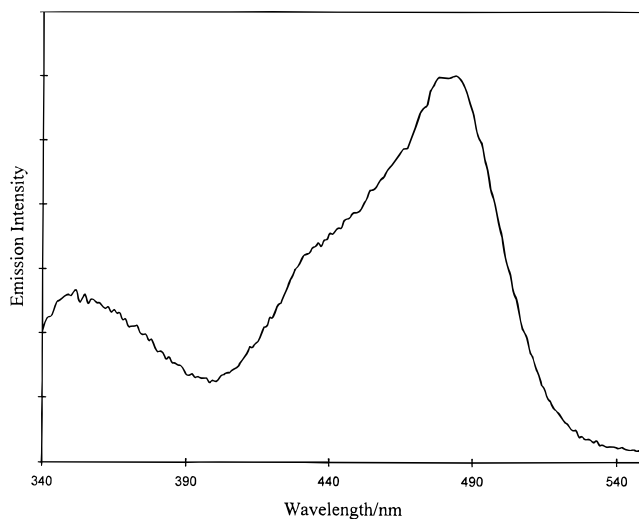


Figure 6. Excitation spectrum of $[\text{Pt}_2(\mu\text{-dppm})_2(\text{C}\equiv\text{CBp})_3]\text{PF}_6$ in degassed CH_3CN at 298 K monitored at 640 nm.

($\text{C}\equiv\text{CPh}$) transition in the monomeric $[\text{Pt}(\text{dppm})_2(\text{C}\equiv\text{CR})_2]$ complex, where $d\sigma^*$ is the antibonding combination resulting from the interaction of the $\text{Pt}(5d_z^2)-\text{Pt}(5d_z^2)$ orbitals, while $p\sigma$ is the bonding combination resulting from the interaction of the $\text{Pt}(6p_z)-\text{Pt}(6p_z)$ orbitals, taking the Pt–Pt bond axis to be the z -axis. In view of the low-lying energy of the π^* orbital of the acetylide ligands, it is not unreasonable to assume the LUMO of the dinuclear complexes to have substantial mixing of the π^* (acetylide) character with the $p\sigma$ orbital arising from the $6p_z-6p_z$ interaction assuming a C_{2v} symmetry (Figure 3).¹⁶ A mixing of the π^* character of terminal carbonyls into the LUMO in A-frame complexes has also been observed.^{2,17} Similar assignments have also been suggested in the related A-frame pyrazolyl-bridged binuclear iridium(I) complexes² and a related $[\text{Pt}_2(\text{dppm})_2(\text{CN})_4]$ system.¹⁸

Excitation of solid samples and fluid solutions of complexes **1–4** at $\lambda > 350$ nm at room temperature resulted in long-lived intense emission. The photophysical data are summarized in Table 2. All the complexes exhibit a broad emission band centered at *ca.* 570–650 nm. Upon cooling of the samples to 77 K, the emission bands become intensified and narrower with the maxima shifted slightly to lower energy. The solid-state emission spectra of the complexes are depicted in Figure 4. The 77 K solid-state emission spectra of $[\text{Pt}_2(\mu\text{-dppm})_2(\text{C}\equiv\text{CC}_6\text{H}_4\text{Et-}p)_3]^+$, $[\text{Pt}_2(\mu\text{-dppm})_2(\text{C}\equiv\text{CC}_6\text{H}_4\text{OEt-}p)_3]^+$, and $[\text{Pt}_2(\mu\text{-dppm})_2(\text{C}\equiv\text{CBp})_3]^+$ all show vibronically structured bands with progression spacing of *ca.* 2000 cm^{-1} , typical of the $\nu(\text{C}\equiv\text{C})$ stretch in the ground state (Figure 5). The observation of the vibronic structures is suggestive of the involvement of the acetylide in the transition. A comparison of the 77 K solid-state emission energy of the complexes shows that the transition energies follow

(16) An assumption of a C_{2v} symmetry for the A-frame complexes is reasonable as a result of the extremely facile “windscreen wiper” action of the bridging acetylide ligand as depicted in Scheme 1.

(17) Hoffman, D. M.; Hoffmann, R. *Inorg. Chem.* **1981**, *20*, 3543.

(18) Yip, H. K.; Lin, H. M.; Cheung, K. K.; Che, C. M.; Wang, Y. *Inorg. Chem.* **1994**, *33*, 1644.

(19) Marshall, J. L.; Stobart, S. R.; Gray, H. B. *J. Am. Chem. Soc.* **1984**, *106*, 3027.

Table 3. Rate Constants for the Quenching of the Excited State of Complexes 1–3 by a Series of Pyridinium Acceptors in Degassed Acetonitrile (0.1 mol dm⁻³ of ⁿBu₄NPF₆) at 25 °C

quencher ^a	<i>E</i> (Q ⁺⁰) ^b vs SCE	<i>k_q</i> /dm ³ mol ⁻¹ s ⁻¹			
		1	2	3	4
3,4-dicyano- <i>N</i> -methylpyridinium	-0.06	4.29 × 10 ⁹	3.88 × 10 ⁹	3.71 × 10 ⁹	3.83 × 10 ⁹
2-chloro-3-nitro- <i>N</i> -methylpyridinium	-0.09	1.79 × 10 ⁹	1.72 × 10 ⁹	1.73 × 10 ⁹	9.62 × 10 ⁸
4-cyano- <i>N</i> -methylpyridinium	-0.67	9.64 × 10 ⁸	1.02 × 10 ⁹	9.87 × 10 ⁸	4.05 × 10 ⁸

^a Except for 4-cyano-*N*-methylpyridinium being a hexafluorophosphate salt, all other compounds are tetrafluoroborate salts. ^b From ref 19.

the order **4** < **5** < **1** ≤ **2** ≤ **3** < **6**, which is in line with the increasing π* orbital energy of the acetylide ligand. This further supports the involvement of the π*(C≡CR) orbital in the transition.

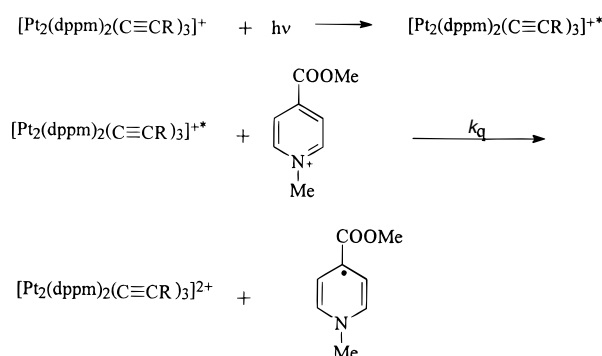
The emission spectra of the complexes in degassed dichloromethane or acetonitrile also showed low-energy emission bands which are symmetric, broad, and intense and are centered at ca. 620–640 nm. The long luminescence lifetimes in the microsecond range together with the large Stokes shift are suggestive of their phosphorescent nature.

The excitation spectra of the complexes monitored at the emission maxima show excitation maxima well correlated with the absorption maxima of the corresponding complexes. The resemblance of the excitation spectra to the absorption spectra suggests that the emissive state is likely to be derived from a MMLCT origin. The excitation spectrum of [Pt₂(μ-dppm)₂(C≡CBp)₃]PF₆ shows two excitation bands at ca. 430 and 480 nm in degassed acetonitrile, tentatively assigned as the ¹[(dσ*)²] → ¹[(dσ*)¹(pσ/π*)¹] (singlet–singlet) and ¹[(dσ*)²] → ³[(dσ*)¹(pσ/π*)¹] (singlet–triplet) transitions (Figure 6). The observed energy separation of ca. 2420 cm⁻¹ between the singlet–singlet and singlet–triplet transitions is similar to an energy separation of 2198 cm⁻¹ for the ¹A₁ → ¹B₁ and ¹A₁ → ³B₁ transitions and 2535 cm⁻¹ for the ¹A₁ → ¹A₁ and ¹A₁ → ³A₁ transitions in the related Ir₂(μ-3,5-Me₂pz)₂(CO)₄ complex in 2-methylpentane at room temperature (3,5-Me₂pz = 3,5-dimethylpyrazole).²

Although the involvement of the π*(C≡CR) orbital in the excited state and the trend in the emission energies upon changing the nature of the acetylide could also be suggestive of an origin derived from an emissive state of intraligand π → π*(C≡CR) character, such an assignment is not favored on the grounds that intraligand π → π*(C≡CR) transitions do not usually occur at such low energies. Moreover, a comparison of the emission energies for the dinuclear A-frame complexes with the corresponding monomeric [Pt(dppm)₂(C≡CR)₂] counterparts shows a red shift in emission energy upon going from the mononuclear species to the dinuclear complexes. An origin of pure π → π*(C≡CR) transition would predict similar emission energies for both the monomeric and the dinuclear complexes. Therefore, a MMLCT origin for the emission is favored. This has

also been supported by resonance Raman spectroscopic studies on complex **5**.⁹ The resonance Raman spectra of complex **5** have very similar relative intensities and resonantly enhanced features as the corresponding monomeric complex MLCT resonance Raman spectra.⁹ This also lends additional support for the assignment of the ca. 380 nm absorption transition of the dinuclear platinum acetylide complexes to an MMLCT transition and not to an intraligand transition (π → π* on the C≡CR). Bands at similar energies have also been shown to exhibit large metal-to-ligand charge transfer (MLCT) character in the related A-frame dinuclear iridium(I) complexes.²

Bimolecular quenching rate constants for the various complexes with different pyridinium quenchers are listed in Table 3. The quenching rate constants generally increase with an increasingly less negative reduction potential of the quenchers. An oxidative electron transfer mechanism has been suggested for the quenching reaction:



Transient absorption bands at ca. 390 nm characteristic of the pyridinyl radicals are observed, confirming the electron transfer nature of the quenching reactions.

Acknowledgment. We acknowledge financial support from the Research Grants Council, The University of Hong Kong, and the State Key Laboratory of Coordination Chemistry of Nanjing University, L.-P.C., P.K.-Y.Y., and K.-L.Y. the receipt of a postgraduate studentship, administered by The University of Hong Kong.

OM971021D